Undrained Bearing Capacity of Unsaturated Soils

D.W. Rassam
PhD Candidate, The University of Queensland, Australia
D.J. Williams
Associate Professor of Geomechanics, The University of Queensland, Australia

Summary The development of matrix suctions in soils contributes to their shear strength, resulting in an enhanced factor of safety against bearing capacity failures. A ϕ=0 bearing capacity analysis carried out to investigate the effect of matrix suctions is described in this paper. The contribution of matrix suction to shear strength is interpreted as an additional cohesion for use in bearing capacity calculations. The cohesion of soil is described by three components: a constant cohesion value corresponding to a matrix suction of zero, and two other components defining a bi-linear shear strength envelope that is dependent on the air-entry value and the de-saturation conditions whether hydrostatic or evaporative. Shear strength profiles were estimated by coupling predicted matrix suction profiles obtained from a one-dimensional numerical model of evaporation and experimental unsaturated-undrained shear strength data. An enhanced bearing capacity was obtained that was dependent on the water table depth and the duration of the evaporation.

1. INTRODUCTION

The contribution of matrix suction to the shear strength of unsaturated soils has attracted increased attention in recent research. Accounting for this contribution to the shear strength of soils results in an enhanced factor of safety in bearing capacity calculations. Rahardjo et al. (1995) illustrated the importance of matrix suctions in the instability of a residual soil slope in Singapore, where shallow slides are very common. Oloo et al. (1997) concluded that matrix suction can have a significant effect on the bearing capacity of pavement structures. Rassam and Williams (1997) predicted the matrix suction and shear strength profiles of a desiccated tailings deposit under hydrostatic and evaporation conditions. They demonstrated that the stability was enhanced by up to 28% when the matrix suction contribution to shear strength was taken into account in the calculations.

In this paper, the undrained bearing capacity of a desiccated soil is estimated, accounting for the contribution of matrix suction to its shear strength. The solution utilises the Fellenius method (Taylor, 1948). It assumes a simple circular slip analysis, and is a modification of the method proposed by Button (1953). The matrix suction profiles of a desiccating soil deposit following various periods of evaporation are predicted using a one-dimensional numerical model that simulates unsaturated water flow in both liquid and vapour phases. The undrained shear strength profile of the desiccated soil is estimated by coupling the predicted suction profiles and the experimentally determined undrained shear strength envelope.

The soil properties used in the analysis are those of Indian Head till, which comprises 28% sand, 42% silt, and 30% clay. The saturated hydraulic conductivity of this soil was assigned a value based on its particle size distribution. All soil parameters were obtained from Vanapalli (1994).

2. SHEAR STRENGTH OF UNSATURATED SOILS

For unsaturated soils, Fredlund et al. (1978) proposed the linear shear strength relationship:

$$\tau = c' + (\sigma_n - u_a)\tan\phi' + (u_a - u_w)\tan\phi^b \quad (1)$$

where τ is the shear strength of the unsaturated soil, c' is the effective cohesion of the same soil when saturated, ϕ' is the effective angle of shearing resistance of the saturated soil, ϕ^b is the angle of shearing resistance with respect to matrix suction, $\sigma_n - u_a$ is the effective normal stress at failure (the difference between normal stress and pore air pressure), and $u_a - u_w$ is the matrix suction of the soil (the difference between pore air and pore water pressure). This relationship is basically an extension of the Mohr-Columb shear strength equation for saturated soils.

In reality, the shear strength envelope with respect to matrix suction may be planar, implying that ϕ^b is constant, or may be curved, implying that ϕ^b varies as a function of matrix suction. Ho and Fredlund (1982), reported a linear increase in strength with respect to matrix suction for two Hong Kong residual soils. A similar trend was observed by Rahardjo et al. (1995) for a residual clay in Singapore. Vanapalli et al. (1996) attributed this

linearity to the fact that the soils tested are resistant to de-saturation and hence can exhibit a linear shear strength behaviour over a large range of suctions. The soil used by Rahardjo et al. (1995) maintained a high degree of saturation up to a suction of 400 kPa and had a ϕ^b value equal to that of ϕ'. Hence, for matrix suctions below the air-entry value (AEV), an increase in matrix suction has the same effect as increasing the effective normal stress. On the other hand, Escario and Saez (1986), Oloo and Fredlund (1996), Vanapalli et al. (1996), and Rassam and Williams (1997) have all reported non-linear shear strength envelopes with respect to matrix suction. Oloo and Fredlund (1996) explained the non-linearity of the shear strength envelope as the result of the diminishing contribution of matrix suction to shear strength as the water content of the soil approaches residual water content.

Thus, in the range of practical matrix suctions employed in the triaxial apparatus (0-500 kPa), we would expect a linear envelope for a fine clayey soil because within this range of matrix suctions, its water content is likely to remain well above the residual value. In Figure 1, soil (a) has an AEV > 500 kPa and a perfectly linear failure envelope with respect to matrix suction. On the other extreme, coarse sandy soils exhibit highly non-linear envelops because they reach their residual water contents at low suctions.

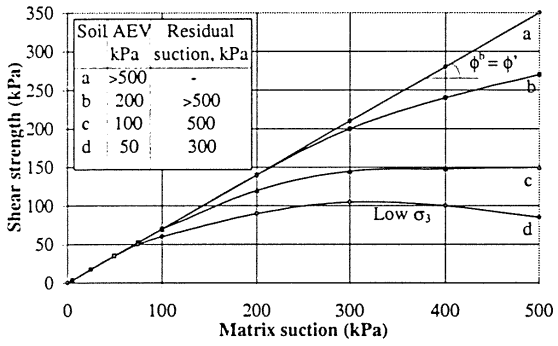

Figure 1. Shape of failure envelope with respect to matrix suction for hypothetical soils.

In general, a failure envelope with respect to matrix suction comprises two parts: a linear portion up to the AEV (Figure 1, soil (b), suction < 200 kPa), where the soil remains saturated, and a non-linear portion as the soil commences to de-saturate (Figure 1, soil (b), suction > 200 kPa). At residual suction, the contribution of matrix suction to the shear strength becomes negligible. That is, the failure envelope flattens progressively, ultimately becoming horizontal, and ϕ^b attains a zero value (Figure 1, soil (c), suction = 500 kPa). Within the range of matrix suctions applied in the triaxial apparatus, the non-linearity of the failure envelope may be related to the AEV. Since the AEV of a soil is dependent on the normal stress acting on it, the extent of the non-linearity would then also be stress-dependent. If soil (c) in Figure (1) is tested at some higher confining pressure, it might exhibit an envelope similar to that of soil (b). At any suction higher than the new AEV and lower than residual, the slope of the failure envelope would increase with the effective confining pressure. Hence, at a higher confining pressure, to attain a zero slope where matrix suction no longer contributes to strength ($\phi^b = 0$), a higher suction would have to be imposed. This means that there is a wider band of matrix suctions where a contribution to strength is available, and hence a higher overall contribution to strength by matrix suctions.

At high matrix suctions, the value of ϕ^b may be positive or negative depending on the rate of de-saturation and on the amount of dilation during shearing. Gan and Fredlund (1996) reported that, at a low confining pressure, ϕ^b could attain a negative value (Figure 1, soil (d)). They attributed this phenomenon to the disruption of the water phase by dilative effects during shearing. They concluded that these effects were more pronounced for coarse materials and that dilation during shearing tended to increase with matrix suction. The shear strength variation with matrix suction in undrained conditions is similar to that under drained conditions (Vanapalli, 1994).

3. NUMERICAL SIMULATION OF EVAPORATION

In the present analysis, the one-dimensional isothermal flow model presented by Campbell (1985) was used to simulate the evaporation process from the surface of a desiccating soil deposit. It models coupled liquid-vapour water flux through the soil.

In an unsaturated soil column, flow is governed by the following non-linear differential equation:

$$k\frac{d^2h}{dz^2} + \frac{dk}{dz}\frac{dh}{dz} = \frac{d\theta}{dt} \qquad (2)$$

where k is the hydraulic conductivity, h is the total head, z is the dimension in the direction of flow, θ is the volumetric moisture content, and t is the time. Establishing the matrix suction profile of any soil deposit involves coupling Equation (2) with Darcy's law, and solving it using the relevant boundary conditions; in this case, the evaporative flux.

Solving the differential equations of unsaturated flow requires a knowledge of the soil-water characteristic curve (WCC), and the hydraulic conductivity function of the soil. The following simple function was used to model the WCC.

$$\psi_m = \psi_e\left(\frac{\theta}{\theta_s}\right)^{-b} \qquad (3)$$

where ψ_m is matrix suction, ψ_e is the air-entry value, θ_s is the saturated volumetric moisture content, and b is the slope of the $\log(\psi_m)$ versus $\log(\theta)$ curve. The values of ψ_e and b are found by plotting moisture release data to log-log scales and fitting a straight line to the data. The slope and intercept of the best-fit line are used to find ψ_e and b.

The following unsaturated hydraulic conductivity function was given by Campbell (1974).

$$k = k_s\left(\frac{\psi_e}{\psi_m}\right)^{2+\frac{3}{b}} \tag{4}$$

where k_s is the saturated hydraulic conductivity. The relationships and fitting parameters for the WCC and hydraulic conductivity function of the Indian Head till are shown in Figure 2.

The flux density of vapour is described by Fick's law:

$$f_v = -D_v\frac{dc_v}{dz} \tag{5}$$

where D_v is the vapour diffusivity of soil (m^2/sec). It depends upon the diffusivity of the vapour through air, the soil porosity, and the volumetric air content. The vapour concentration c_v is given by

$$c_v = H_r c_v' \tag{6}$$

where H_r is the relative humidity and c_v' is the saturation vapour density (0.017 kg/m3 at 20°C). The relationship between humidity and total suction is given by the following relationship:

$$H_r = \exp\left(\frac{M_w\psi_t}{\Theta R\rho_w}\right) \tag{7}$$

where M_w is the mass of a mole of water (0.018 kg/mol), ψ_t is the total soil suction (-Pa), R is the gas constant (8.3143 J/mole K), Θ is the absolute temperature (°K), and ρ_w is the density of water (kg/m^3).

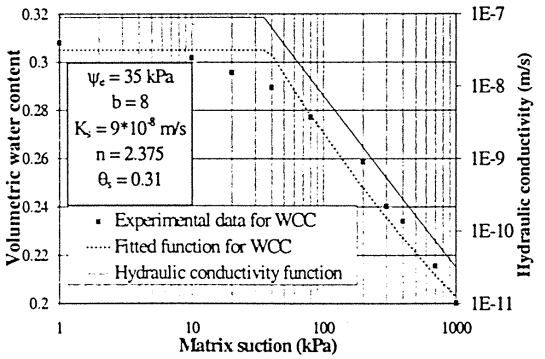

Figure 2. Soil-water characteristic curve and hydraulic conductivity function.

The flux boundary condition at the soil surface is the actual evaporation rate E_a. This may be estimated by means of the following expression (Campbell, 1985):

$$E_a = \frac{H_s - H_a}{1 - H_a}E_p \tag{8}$$

where E_p is the potential or pan evaporation rate, H_s is the humidity at the soil surface, and H_a is the atmospheric humidity (assumed to be 50%). Wilson et al. (1997) reported that the results obtained using Equation (8) compared well with measured experimental data, hence confirming its validity.

The lower boundary condition is the water table represented by a constant potential equal to the AEV. The model is capable of modelling flow in the unsaturated zone. That is, the soil's potential must be equal to or lower than the AEV.

Evaporation was simulated for a soil deposit where the depth of the unsaturated zone D_{US} was 5 m. The initial potential profile was a constant potential equal to AEV. Potential evaporation E_p was assigned a value of 10 mm/day. The results are shown in Figure 3. As evaporation proceeds, matrix suctions increase especially at the surface until they reach a steady state condition. The time required to reach this condition is dependent on the evaporation rate, D_{US}, and the hydraulic and water retention properties of the soil.

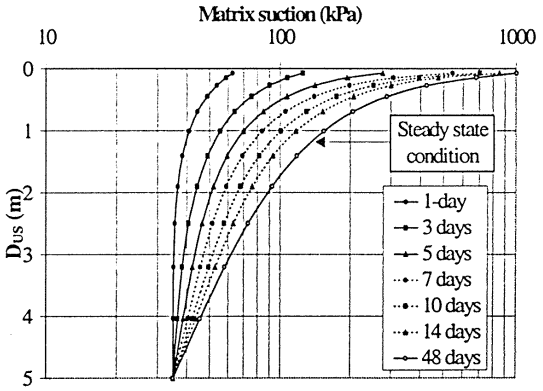

Figure 3. Matrix suction profiles after various evaporation periods.

4. SHEAR STRENGTH PROFILES

Vanapalli (1994) established the undrained shear strength envelope with respect to matrix suction for the Indian Head till (Figure 4). The experimental envelope was coupled with the predicted matrix suction profile to yield the shear strength profile of the soil. Figure 5 shows the shear strength profile for hydrostatic conditions. For a water table depth of 3.5 m (equal to AEV), the shear strength varies linearly from C_o at the water table surface (the undrained shear strength at zero matrix suction), to

C_o+C_{AEV} at the surface, where C_{AEV} is the strength at a matrix suction equal to AEV. At deeper water tables, the profile starts to deviate from a straight line at a height equal to AEV above the water table. The shear strength profiles for evaporative conditions are shown in Figure 6. The initial strength is that corresponding to the initial potential (AEV). The residual matrix suction is around 250 kPa (Figure 4), and beyond this suction the shear strength is assumed to be remain constant. For the bearing capacity analysis, the strength profiles shown in Figures 5 and 6 were approximated by bi-linear profiles.

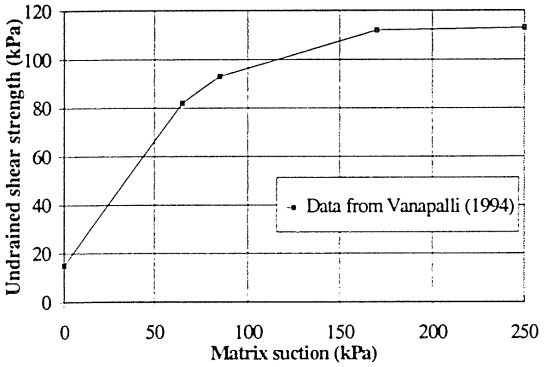

Figure 4. Unsaturated-undrained shear strength data.

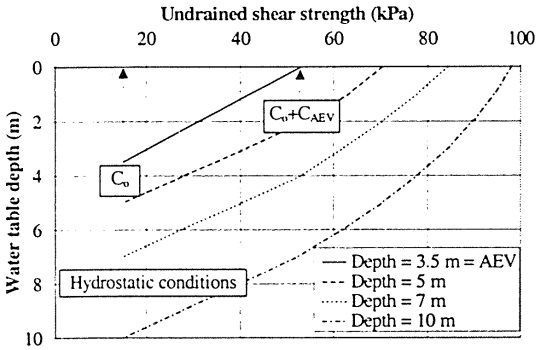

Figure 5. Shear strength profile for hydrostatic conditions.

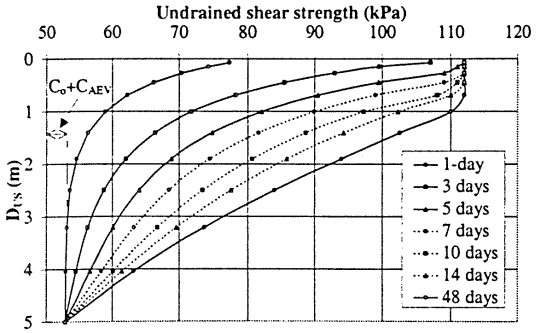

Figure 6. Shear strength profiles after various evaporation periods.

5. BEARING CAPACITY ANALYSIS

The undrained bearing capacity is given by:

$$q_{ult} = C_u N_c \tag{9}$$

where q_{ult} is the ultimate bearing capacity, C_u is the undrained shear strength, and N_c is a dimensionless bearing capacity factor equal to 5.14 for a long rectangular foundation at the ground surface. Button (1953) was the first to analyse footings on layered soils of different cohesions and zero angle of internal friction. Assuming a simple circular slip surface, he provided charts for the bearing capacity factor N_c for a footing on the surface of a layer of cohesion C_1 underlain by a thick layer of cohesion C_2, and for a footing on the surface of a layer in which the cohesion varies linearly with depth from C_1 at the surface to C_2 at a depth d and underlain by a thick layer of cohesion C_o. The condition of limiting equilibrium is obtained by calculating moments about the centre of a circular failure surface. For the special case of a homogeneous profile, the solution procedure gives a value of N_c of 5.51. Reddy and Srinivasan (1967) further modified the method proposed by Button (1953) to include the nonhomogeneity and isotropy of soil with respect to shear strength.

Oloo et al. (1997) used a limit equilibrium method for bearing capacity in layered soils with incorporation of matrix suction for the design of unpaved roads. They reported that since matrix suction does not have a gravitational component, its influence on the stability of the soil under the footing will arise from its contribution to the shear strength of the soil. Matrix suction contribution to the shear strength is usually interpreted as an additional cohesion to the shear strength profile above the water table.

In this paper, the solution proposed by Button (1953) is modified to accommodate two finite layers of soil with thicknesses D_2 and D_1 and linearly varying cohesion, resting on an infinite layer of constant cohesion equal to the undrained shear strength of the soil. Assuming a circular slip surface with centre O, the limiting equilibrium is obtained by summing the moments of the forces around O (Figure 7):

$$\begin{aligned} 2q_{ult}\,b\left[r\sin(\theta)-b\right] = {} & 2r^2\theta C_o + 2r^2 C_1(\theta-\gamma) + \\ & 2\int_{\psi}^{\gamma} r^2 \frac{C_1}{D_1}\left[r\cos(\psi)-r\cos(\alpha)\right]d\alpha + \\ & 2\int_{\gamma}^{\theta} r^2 \frac{C_2}{D_2}\left[r\cos(\gamma)-r\cos(\alpha)\right]d\alpha \end{aligned} \tag{10}$$

$$= 2r^2 \left\{ \begin{array}{l} \theta C_o + C_1(\theta - \gamma) \\ + \dfrac{C_1 r}{D_1}\left[(\gamma - \psi)\cos(\psi) - \sin(\gamma) + \sin(\psi)\right] \\ + \dfrac{C_2 r}{D_2}\left[(\theta - \gamma)\cos(\gamma) - \sin(\theta) + \sin(\gamma)\right] \end{array} \right\}$$

where b is half the width of the foundation, r is the radius of the slip surface, D_2 and D_1 are the thicknesses of the top and lower soil layers respectively, C_o is the undrained shear strength of soil, C_1 and C_2 represent the contribution of matrix suction to shear strength estimated from a bi-linear approximation of the shear strength envelope, θ is the angle (expressed in radians) defining the circular soil failure surface, ψ is the angle (expressed in radians) defining a segment of the circular failure surface that passes through the lowermost soil layer, γ is the angle (expressed in radians) defining a segment of the circular failure surface that passes through the two lower soil layers, and α is an integration variable. The target minimum bearing capacity is that which satisfies:

$$\frac{\partial q_{ult}}{\partial \theta} = \frac{\partial q_{ult}}{\partial r} = 0 \qquad (11)$$

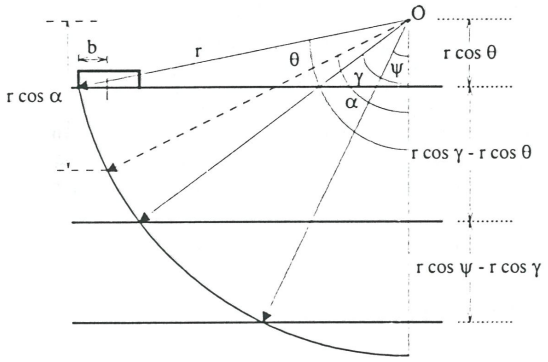

Figure 7. Slip circle bearing capacity analysis.

The procedure of minimising q_{ult} is demonstrated for a hypothetical problem in Figure 8. The bearing capacity is plotted versus r, and a family of curves are produced for various θ values. The set of values that result in the absolute minimum are those which satisfy Equation 9.

Referring to Figure 9a, the depth D_2 is equal to AEV. Under hydrostatic conditions, matrix suction changes linearly with depth, as does the shear strength envelope up to AEV. Therefore, the bi-linear approximation of the shear strength envelope should have its intersection point at a suction equal to AEV. Under evaporative conditions, the matrix suction profile is non-linear and the intersection

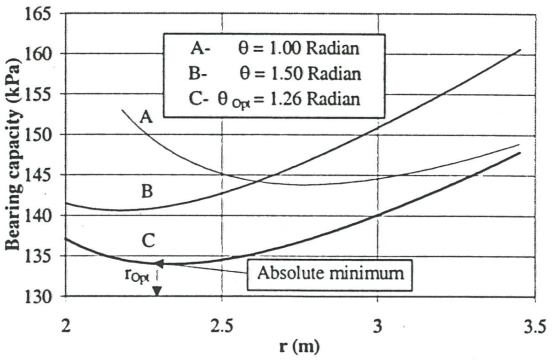

Figure 8. Minimising angle and radius of circular slip circle.

point changes location depending on the duration of the evaporation. The cohesion of the lowermost layer is composed of two constant parts. The first is C_o, the undrained shear strength at zero matrix suction, and the second is C_{AEV}, the contribution of matrix suction to the undrained shear strength that corresponds to a matrix suction equal to the AEV (Figure 9b). All bearing capacity analyses are based on a footing with a half width of 2 m.

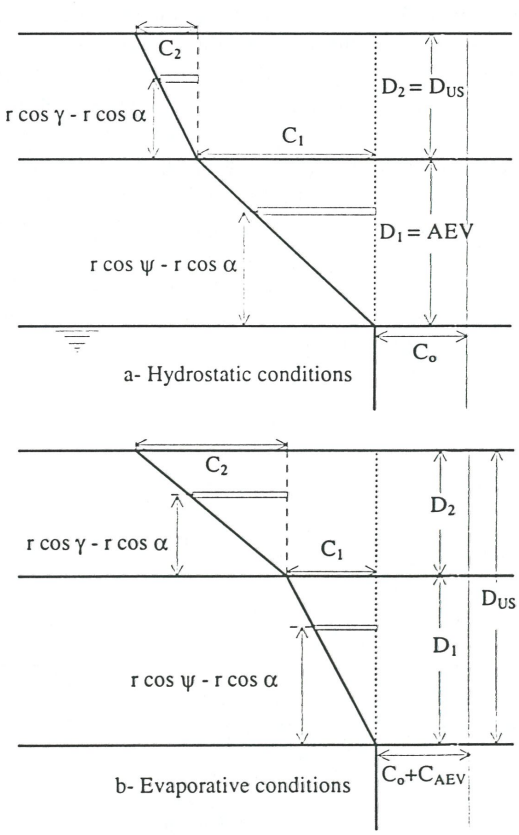

Figure 9. Bi-linear shear strength profiles for hydrostatic and evaporative conditions.

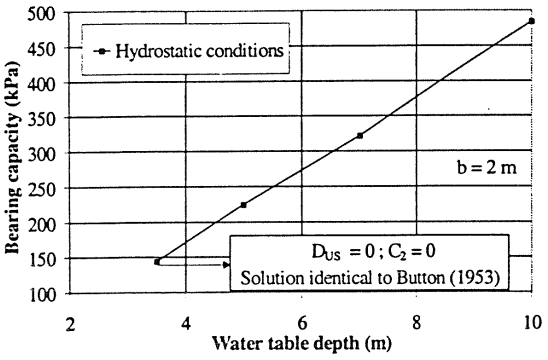

Figure 10. Bearing capacity for various water table depths under hydrostatic conditions.

The results of the bearing capacity analysis corresponding to the shear strength profiles for hydrostatic conditions are shown in Figure 10. At a water table depth equal to AEV, D_{US} and C_2 are both zero, and the problem reduces to that solved by Button (1953). As the water table increases, the bearing capacity increases linearly with depth. For a water table depth of 10 m, the bearing capacity is increased five-fold over that of the case where matrix suctions are neglected.

The results of the bearing capacity analysis corresponding to the shear strength profiles for evaporative conditions are shown in Figure 11. The initial bearing capacity for zero evaporation time corresponds to that for a homogeneous soil with cohesion $C_u = C_o + C_{AEV}$, and is equal to $5.5C_u$. As evaporation proceeds, a sharp initial increase in bearing capacity occurs due to the desiccation of the near-surface soil. At later stages, the increase slows until the bearing capacity reaches a maximum constant value at steady state evaporative conditions. The matrix suction profile of the soil then remains unchanged.

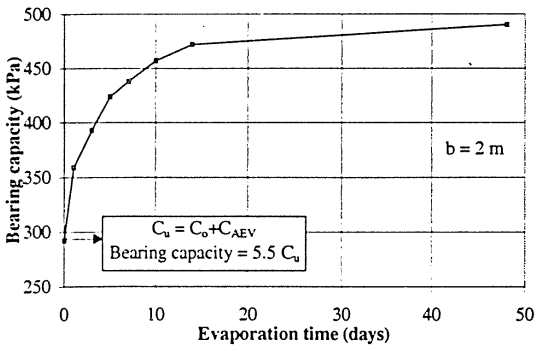

Figure 11. Bearing capacity after various evaporation periods.

6. CONCLUSIONS

The contribution of matrix suction to the shear strength of unsaturated soils results in a significantly enhanced bearing capacity. For hydrostatic conditions, matrix suctions vary linearly with depth. Hence, the failure envelope with respect to matrix suction comprises two segments: the first is linear up to a suction equal to the air-entry value and the second is non-linear. For evaporative conditions, the matrix profile is non-linear and varies with the depth of the unsaturated zone, the evaporation rate, and the duration of the evaporation. For both conditions, the shear strength profile may be approximated by a bi-linear envelope that is dependent on the air-entry value and the de-saturation conditions whether hydrostatic or evaporative.

A simple circular slip surface bearing capacity analysis has been described that accounts for matrix suctions. It is a modification of the method proposed by Button (1953). The soil is discretised into three layers. The lowermost layer, which is assumed to extend to infinite depth, has a constant cohesion equal to the undrained shear strength of the soil. The second and the third layers, which are both of finite depths, have cohesions that vary linearly with depth.

The bearing capacity analysis has confirmed the importance of incorporating the effects of matrix suctions into the calculations. For hydrostatic conditions, accounting for the contribution of matrix suction to the shear strength resulted in a five-fold increase in the bearing capacity when the water table was located at a depth of 10 m. For evaporative conditions, a sharp increase in bearing capacity was noted during the initial desiccation, followed by a slow increase which ultimately ceased when steady state evaporative conditions were reached.

7. REFERENCES

Button, S.J. (1953). The bearing capacity of footings on a two-layer cohesive subsoil. *Proceedings of the 3rd International Conference on Soil Mechanics and Foundation Engineering*, Zurich, Switzerland, Vol. 1, pp. 332-335.

Campbell, G. S. (1974). A simple method for determining unsaturated conductivity from moisture retention data. *Soil Science*, Vol. 117, pp. 311-314.

Campbell, G. S. (1985). *Soil Physics with BASIC*. Elsevier, New York.

Escario, V. And Saez, J. (1986). The Strength Of Partly Saturated Soils. *Geotechnique*, Vol. 36, No. 3, pp. 453-456.

Fredlund, D.G. and Rahardjo, H. (1993). *Soil Mechanics for Unsaturated Soils*. John Wiley and Sons, New York.

Fredlund, D.G., Morgenstern, N.R. and Widger, R.A. (1978). The shear strength of unsaturated soils. *Canadian Geotechnical Journal*, Vol. 15, pp. 313-321.

Gan, J.K. and Fredlund, D.G. (1996). Determination of the shear strength parameters of an unsaturated soil using the direct shear test. *Canadian Geotechnical Journal*, Vol. 25, pp. 500-510.

Ho, D.Y.F., and Fredlund, D.G. (1982). Increase in strength due to suction for two Hong Kong Soils. *Proceedings of the ASCE Geotechnical Engineering Division Specialty Conference*, Honolulu, Hawaii, pp. 263-295.

Oloo, S.Y. and Fredlund, D.G. (1996). A method for determination of ϕ^b for statically compacted soils. *Canadian Geotechnical Journal*, Vol. 33, pp. 272-280.

Oloo, S.Y., Fredlund, D.G., and Gan, J.K. (1997). Bearing capacity of unpaved roads. *Canadian Geotechnical Journal*, Vol. 34, pp. 398-407.

Rahardjo, H., Lim, T.T., Chang, M.F. and Fredlund, D.G. (1995). Shear-strength characteristics of a residual soil. *Canadian Geotechnical Journal*, Vol. 32, pp. 60-77.

Rassam, D.W. and Williams, D. J. (1997). Shear strength of unsaturated gold tailings. *Proceedings of the 1st Australia-New Zealand Conference on Environmental Geotechnics*, Melbourne, Australia, pp. 469-474.

Reddy, A.S., and Srinivasan, R.J. (1967). Bearing capacity of footings on layered clays. *Journal of Soil Mechanics and Foundation Division, ASCE*, Vol. 93, No. SM2, pp. 83-92.

Taylor, D.W. (1948). *Fundamentals of Soil Mechanics*. John Wiley and Sons, New York.

Vanapalli, S.K. (1994). *Simple tests procedures and their interpretation in evaluating the shear strength of unsaturated soils*. Ph.D. thesis, University of Saskatchewan, Saskatoon, Canada.

Vanapalli, S.K., Fredlund, D.G., Pufahl, D.E., and Clifton, A.W. (1996). Model for the prediction of shear strength with respect to soil suction. *Canadian Geotechnical Journal*, Vol. 33, pp. 379-392.

Wilson, G.W., Fredlund, D.G., and Barbour, S.L. (1997). The effect of soil suction on evaporative fluxes from soil surfaces. *Canadian Geotechnical Journal*, Vol. 34, pp. 145-155.